REVIEW

The Solar Wind–Magnetosphere–Ionosphere System

John G. Lyon

The solar wind, magnetosphere, and ionosphere form a single system driven by the transfer of energy and momentum from the solar wind to the magnetosphere and ionosphere. Variations in the solar wind can lead to disruptions of space- and ground-based systems caused by enhanced currents flowing into the ionosphere and increased radiation in the near-Earth environment. The coupling between the solar wind and the magnetosphere is mediated and controlled by the magnetic field in the solar wind through the process of magnetic reconnection. Understanding of the global behavior of this system has improved markedly in the recent past from coordinated observations with a constellation of satellite and ground instruments.

An unseen electrical generator, more powerful than any man-made generator, exists in space near Earth. Day after day, this generator produces as much as hundreds of billions of watts, about equal to the generation capacity of North America. This generator is at the heart of the integrated solar wind, magnetosphere, and ionosphere system. The driver for this generator is the solar wind, the tenuous ionized gas that flows outward from the sun with speeds of hundreds of kilometers per second. The energy transported by this wind is only one-millionth of the sun's total radiation. Still, enough is transferred to Earth and near-Earth space to be comparable to man-made energy production. Earth's magnetic field acts as the wires to transmit the solar wind energy to the ionosphere, where the energy is dissipated mainly as heat, and to accelerate charged particles circling fairly close to Earth. The ionosphere in the Arctic and Antarctic regions acts as the primary resistor. Side effects of this circuit lead to the aurorae and to variations in Earth's radiation belts.

Variations in the solar wind cause changes throughout the region about Earth, in the ionosphere, and at the ground. These changes have been called space weather. Space weather can have serious practical consequences (*1*, *2*). Changes in the currents flowing through the ionosphere can cause disruption to power distribution systems, long-line telephone networks, and corrosion of pipelines on the ground (*3*). Changes in the radiation environment near Earth can seriously affect satellite operation near Earth through spacecraft charging and generation of false commands (*4*, *5*). The peak of the solar cycle occurs later this year; the increased activity level within the 3 years around the peak will bring more and stronger events capable of disrupting geospace, the space environment in the vicinity of Earth. The importance of predicting the geospace environment has been stressed by the formation of the National Space Weather Program (*6*).

Department of Physics and Astronomy, Dartmouth College, Hanover, NH 03755, USA.

Earth's magnetic field is a barrier to the solar wind, which is diverted around Earth. The region where Earth's field dominates is the magnetosphere (Fig. 1). Earth's magnetic field is sufficiently strong that it can usually keep the solar wind from approaching closer than about 10 Earth radii (R_E) on the front side. The solar wind in turn confines Earth's magnetic field on the dayside. On the nightside, Earth's magnetic field expands into the lower pressure region, forming the magnetotail. The tail consists of regions on either side of the center where the density is low and the magnetic field dominates, the tail lobes. The lobes surround a higher density, lower field region, the plasma sheet. The boundary between the magnetosphere and the solar wind is the magnetopause. Because the flow in the solar wind is almost always supersonic, the collision of the solar wind with the magnetosphere causes a bow shock in the solar wind. The region between the bow shock and the magnetopause is the magnetosheath. Earth's outer radiation belt lies where it is indicated in Fig. 1. The inner belt generally is separated from the outer belt and is about half as far out from Earth.

Magnetic field lines are a mathematical fiction, useful for describing the organization of magnetic fields. But, when embedded in a conducting medium, they attain a real physical importance. Under these conditions, the plasma on a given field line remains tied to that field line as the field and the plasma evolve. In addition, the field lines act as conduits for physical stresses to be transmitted between different regions connected by the field lines. If field lines always maintained their integrity, the interaction of Earth's field with the solar wind would be uninteresting. Earth's field would be confined by the solar wind, and little energy would flow from the solar wind to the magnetosphere. However, when regions with differently directed magnetic fields come in contact, it is possible for magnetic field lines to reconnect (Fig. 2). Oppositely directed magnetic fields join, leading to field lines with plasma from the two different regions now on the same field line. The magnetic field topology has been changed to permit direct linkage between the two regions. Dungey (*7*) first sketched the consequences for an interplanetary (solar wind) magnetic field (IMF) that was oppositely directed (southwardly) from the generally northward terrestrial field. Magnetic field lines that are connected only to Earth are termed closed. Reconnection occurs on the dayside, turning closed field into open field lines (that is, one end connected to Earth and the other in the solar wind). The reconnected, open field lines take part in the antisunward motion of the solar wind and get dragged to the nightside where the field enhances the tail lobes. To maintain a steady state, reconnection must again occur on the nightside, and the now closed field line must return to the dayside. Thus, reconnection gives rise to convection of plasma through the magnetosphere. Magnetic field lines start at the dayside, reconnect, and are dragged into the tail. After reconnection in the tail, they convect in the interior of the magnetosphere in a generally sunward direction until they return to the dayside. The Earth-ward ends of the field lines undergoing convection lie in the ionosphere. The plasma in the ionosphere coexists with the neutral atmosphere. Collisions between the neutral atoms and molecules and the ions limit how quickly the ions can respond to magnetospheric convection. This collisional drag forces momentum to flow from the solar wind plasma on open field lines to the ionosphere and currents to flow within the ionosphere (Fig. 2C). Across the top of the polar cap, the flow is away from the sun, returning to the dayside at lower latitudes on both the dawn and dusk sides. This is the common two-cell ionospheric convection pattern (Fig. 2C). The energy for ionospheric and magnetospheric convection is extracted from the kinetic energy of the solar wind flow, particularly the flow at the boundary of the magnetosphere and magnetosheath above and behind the polar caps.

Geomagnetic storms occur when the magnetospheric convection is enhanced, generally by a strong continuous southward IMF. The region where the ionosphere is stirred by the convection moves to lower latitudes, bringing the effects of the currents to more highly populated regions. The energetic flux in the radiation belts is also enhanced. Storms can last from hours to days. Substorms are a shorter, impulsive release of energy and may or may not be a feature of storms. They occur because the reconnection that brings open flux back to the dayside may not be in equilibrium with the dayside reconnection. If more flux is carried to the nightside than is returned, the strength of the tail lobes is increased, storing magnetic energy. This energy can then be released explosively, causing high-speed flows in the magnetotail, relaxation of the magnetic field toward a more dipolar configuration, and auroral displays and intense ionospheric currents. The substorms also lead to the injection of high-energy particles that can build up the radiation belts.

The storm of January 1997 was a moderate sized event typical of conditions during the start of the current solar cycle [see (*8*) for an overview]. What was unusual was the quick tracking of the event by a wide variety of satellites and ground-based observatories. Here I will use this storm to highlight some of the most recent advances in our understanding of the solar wind–magnetosphere–ionosphere system.

The storm was caused by a coronal mass ejection (CME) that was observed by the SOHO (SOlar and Heliospheric Observatory) satellite on 7 January (*9*). The effects of this event began to be felt in the near-Earth region early on 10 January when an interplanetary shock was observed in the solar wind at satellites upwind from Earth (SOHO and WIND—so called for its mission to observe the solar wind). The WIND satellite was closer to Earth and specifically instrumented to observe the solar wind magnetic field and plasma speed and density, quantities that determine much of the geomagnetic effect of the solar wind. The shock wave was caused by the CME running into the ambient solar wind. A few hours after the shock wave was observed, the actual CME arrived in the form of a magnetic cloud. Magnetic clouds are a common subset of CMEs observed at 1 astronomical unit and are characterized by a lower than average solar wind plasma temperature and a smooth rotation of a relatively large magnetic field (two to four times the average) (*10*). The observations are consistent with a well-organized flux rope—a more or less cylindrical region with a magnetic field that is twisted around the central axis, the twist larger toward the outside edge of the cylinder. In the 10 to 11 January cloud, the field was initially southward and rotated over the course of almost a day to northward. The field intensity was three to four times the normal value of about 7 nT during this period. The magnetic cloud was followed by a high-density region thought to be a photospheric filament caught up in the CME (*11*). The pressure of this material forced the magnetopause inside geosynchronous orbit—an unusual occurrence that can cause problems for satellites that use Earth's magnetic field for orientation.

The major magnetic activity associated with this storm occurred during the 10-hour period of strong southward IMF at the leading part of the magnetic cloud. Observations within the magnetosphere of the enhanced convection and other phenomena related to this prolonged southward IMF are at the mercy of the placement of satellites. Even though a fleet of well-instrumented spacecraft has been deployed under the International Solar-Terrestrial Physics (ISTP) program (*12*), the total number of weather stations in space is only a half dozen to cover a volume a million times that of Earth. Nevertheless, reconnection on the dayside was seen during the early part of the southward IMF by the Geotail satellite, which was near the subsolar magnetopause (*13*). Unfortunately, during the initial part of the event, no satellites were positioned to observe tail reconnection. Typically, satellite instruments detect conditions only near the satellite. Recently, more emphasis has been placed on remote sensing. The most time-honored method is to use the ionosphere as a map of what is happening in the magnetosphere. The behavior of reconnection in the magnetotail can then be inferred from a number of measurements, for example, by looking at the boundary between open and closed field lines in the ionosphere (*14*) with an ultraviolet imager on a satellite above the polar cap (open field lines have little particle precipitation and thus do not produce auroral light in the ionosphere). Distant points in the magnetosphere are connected to points in the ionosphere by magnetic stresses that flow along field lines. Observation of the ionosphere, thus, can give a global picture of the magnetosphere. That is partially why there are three different ionospheric imaging systems on the POLAR (*15*) satellite in the visible, ultraviolet, and x-ray regions of the spectrum. The POLAR orbit is eccentric, taking it high over the northern polar cap for panoramic views. In addition, there were ground-based instruments active during the storm. Radars can give direct measurements of the convection velocity in the ionosphere and indirectly give the energy dissipation rate, as did the SuperDARN system during this event (*16*). Ground magnetometers give similar, but complementary, data and were used to provide a comprehensive picture of energy deposition during this event (*17*).

Another new imaging technique that is just beginning to be exploited is energetic neutral atoms (ENAs). It has now become possible to image the magnetosphere directly through detectors sensitive to ENAs (*18*). These atoms are produced by charge exchange between hydrogen atoms of the cool geocorona (*19*) with the hot hydrogen ions.

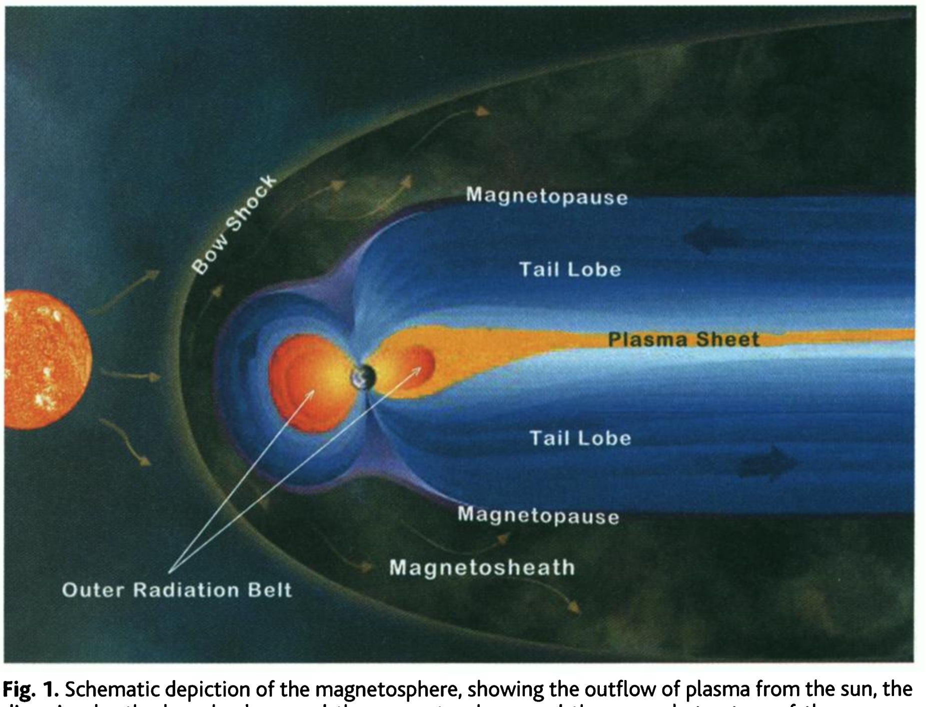

Fig. 1. Schematic depiction of the magnetosphere, showing the outflow of plasma from the sun, the diversion by the bowshock around the magnetosphere, and the general structure of the magnetosphere. The broad blue arrows within the magnetosphere show the direction of the magnetic field.

The net effect is to produce a cool ion and a hot (energetic) atom. Because neutral atoms are not affected by the magnetic field and collisions are rare, the ENAs from distant parts of the magnetosphere can be detected and formed into images. ENA images from the POLAR satellite before the January storm and at its peak (Fig. 3) (*20*) show the formation of the ring current due to the enhanced convection and energetic particle injection during this time. The results are generally consistent with the convection seen at geosynchronous orbit (*21*). The POLAR satellite was not designed to image neutral atoms and the pictures are crude, but they are the first step in a new technology that will be improved in planned future missions. Very recently, on 27 March 2000, the IMAGE satellite was launched. Among its detectors are the first ones specifically designed to image the magnetosphere with ENAs.

Another way of obtaining a global picture is through the use of numerical simulation. The global magnetohydrodyamic (MHD) models (*22*) of the magnetosphere represent the first crude efforts at a first-principles weather prediction model for the space environment. The Geospace Environment Modeling (GEM) program (*23*) has involved both modelers and observers in studies comparing models against comprehensive data sets for steady convection and for substorm conditions [for example, (*24–26*)]. The January cloud was a milestone in that, for the first time, a greater than 24-hour period was simulated with real solar wind data as input (*27*), indicating the feasibility of simulations run in real time as true space weather predictions.

A central problem in magnetospheric physics and for these simulation models is reconnection. Here much recent progress has also been made. The plasma is very nearly collisionless, so normal resistivity is not large enough to produce the observed coupling between the solar wind and the magnetosphere. The early Sweet-Parker model for magnetic reconnection presupposed an elongated, thin current sheet in which reconnection took place (*28*, *29*). Given a finite outflow speed, continuity limited the rate of reconnection to small fractions of the fastest MHD wave speed. Petschek (*30*) was able to show that much more efficient coupling could occur with only a small diffusion region giving rise to fans of slow mode shock waves where the bulk of the energy conversion occurred. Unfortunately, the nature of the dissipation required for reconnection was still not found, and MHD simulations showed that analogs of the magnetospheric system evolved into thin current sheets like the Sweet-Parker model. These current sheets allow reconnection too slow for strong coupling. Furthermore, observations of the dayside reconnection, such as (*13*), are consistent with Petschek's picture, not that of the Sweet-Parker model. In the past few years, attention has focused on the differing length scales associated with the ions and the electrons in the plasma. The heavier ions become decoupled from the electrons at scale lengths below the ion inertial length, c/ω_{pi}. At this point, the Hall electric field that arises from the difference in bulk velocity of the ions and electrons becomes important in the dynamics. This field is not included in the usual fluid (MHD) treatments of reconnection. A number of different methods were used to simulate this

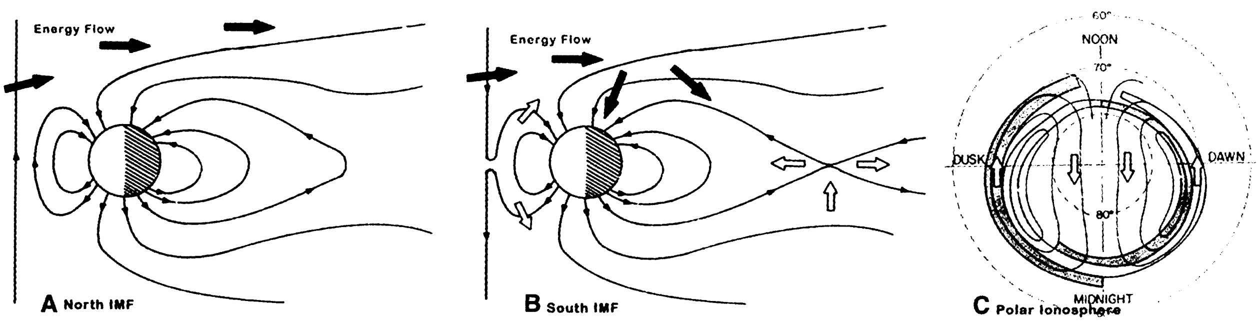

Fig. 2. Schematic of the process of reconnection in the magnetosphere. (**A**) No reconnection and no energy flow into the magnetosphere. Energy flow is indicated by solid arrows. (**B**) Reconnection opens the magnetosphere and allows entry of plasma, momentum, and energy. Magnetospheric convection is indicated by the open arrows. (**C**) The resulting currents and motions in the polar ionosphere for southward IMF. The currents flowing between the nagnetosphere and ionosphere are indicated by the shading: Lighter shading indicates that the current is upward, and darker shading indicates that the current is downward.

Fig. 3. Images of the hot magnetospheric ions seen from above the equatorial plane by the POLAR satellite. The images are smoothed and color-coded by the instrumental count rate, red being higher. The left panel is for a time before the arrival of the CME, and the right panel is toward the end of the period of southward IMF. The time labels in the upper left corner of each panel are month/day of 1997 followed by the universal time.

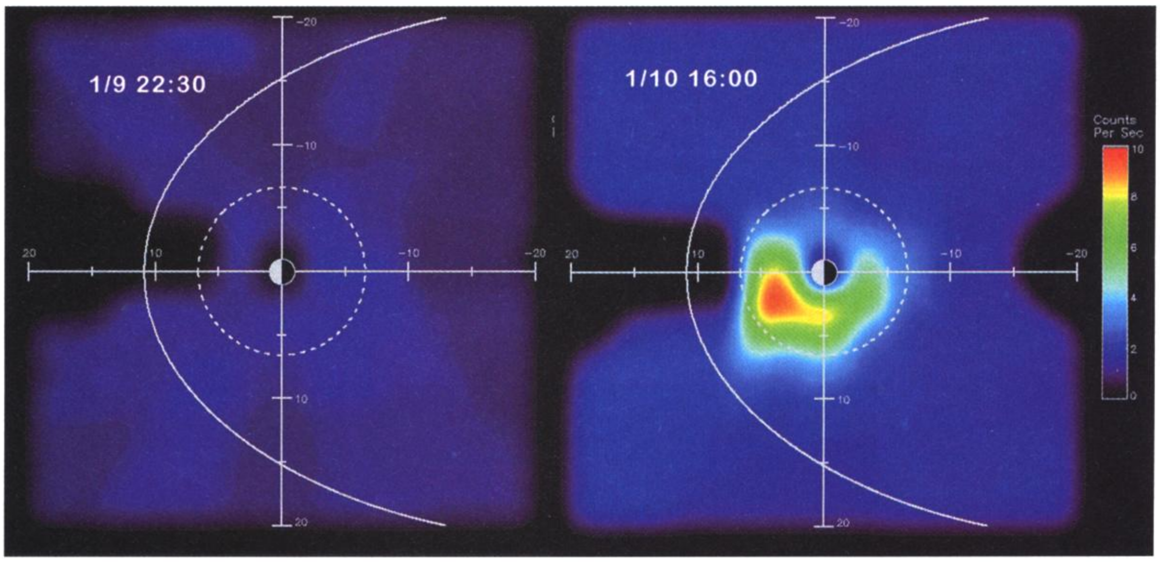

situation, including resistive hybrid simulations (*31*), two-fluid calculations (*32*, *33*), and particle simulations (*34*, *35*). These studies showed that the rate of reconnection was independent of the strength of the dissipation needed to free the electrons from the field lines. In addition, the length of the reconnection region remained quite small, presumably leading to a Petschek-like model in the far field. Figure 4 shows the results of such a calculation (*36*) from a simulation explicitly using electrons and ions. As expected, the ion current pattern is much broader than the electron pattern. This difference in behavior is mediated by whistler waves (*37*), which allow the electrons to be accelerated out of the diffusion region and catch up to the ions. Because of the dispersion character of the whistlers, the resulting reconnection is insensitive to the actual electron dissipation mechanism (*34*). Whistlers are a mode that depends on the existence of a Hall electric field. Removal of the Hall term from these calculations leads to a Sweet-Parker–like reconnection with an extended, thin current sheet.

MHD simulations have generally been successful in modeling the magnetospheric system without the inclusion of this reconnection physics. This is probably luck due to either numerical dissipation that mimics the real process or a resolution that is sufficiently coarse that really thin current sheets cannot form. As part of the GEM program, it was decided to issue a GEM reconnection challenge with the idea of defining what needed to be added to standard MHD models to include realistic reconnection physics. A simplified, but extremely well-defined reconnection problem was set for all who wished to participate with codes ranging from full particle codes to standard MHD codes (*38*). The results showed that all the techniques that included the Hall electric field, whether fluid or particle, gave fast reconnection (flows into the reconnection site ≈0.1 times the fastest MHD wave speed in the system). All the resistive MHD codes gave slow reconnection with extended current sheets. These results show a consistent physical picture for collisionless reconnection. They are also qualitatively consistent with the reconnection in the global MHD codes; adding appropriate reconnection physics to future global models is a realistic goal.

During magnetic storms, the outer radiation belt about Earth is often enhanced in energy flux. The January event showed a large increase occurring over a period of a few hours. This was seen by a number of spacecraft, including GPS (*39*), POLAR (*40*), STRV-1B (*41*), and SAMPEX (*42*). The increase was seen first in the neighborhood of 4 to 5 R_E and later at geosynchronous orbit (*43*). The realization that the radiation belts can respond to solar influence on such a short time scale has been one of the most interesting results of the ISTP era.

There are two ways in which this rapid increase can occur. More rarely, the increase occurs over a short period of time (minutes) associated with storm sudden commencements (SSCs). More commonly, there is a buildup in energetic flux over the course of hours during the main phase of the storm. In the former case, the acceleration mechanism appears to be the interaction of a shock wave in the solar wind with the magnetosphere and the ambient particle populations. Particles of a given energy tend to drift around Earth in fairly regular orbits with a well-defined period. An incoming shock in the solar wind will produce a compression wave through the magnetosphere. If the period of a particle is such that it remains in phase with the electric and magnetic fields of the compression, it can "surf" the wave and be transported inward. This inward motion both brings the particles to the location of the radiation belts and increases their energy in proportion to the change in magnetic field strength from their old position to the new one. The mechanism for the energy increase is analogous to the adiabatic heating of compressed gases. These ideas were first applied to the appearance of new radiation belts after the SSC of 24 March 1991. With the use of a simple analytic model for the compressional fields, remarkable agreement was obtained for the electrons (*44*). The analytic model is not as successful for protons, but fields derived from a global MHD calculation of the fields produced by a shock give substantially better agreement (*45*), as well as good agreement for the electrons (*46*). This mechanism is not common because the wave propagation speed in the magnetosphere is generally high in comparison with the solar wind speed. Thus, most shocks in the solar wind are simply not intense enough to provide the kind of compression needed for this mechanism to operate.

More commonly, increases in radiation belt fluxes during storms occur over hours. Here the mechanism seems to be twofold. First, there are more particles available with energies capable of being accelerated to full radiation belt energy. For electrons, this seed population seems to be mainly due to injection of particles from the tail due to substorms. For the protons, energetic protons in the solar wind are also an important seed population. During the period on 10 January when the increase occurred, the southward IMF produced a number of substorms (*39*). Second, there is enhanced inward diffusion of the energetic populations. For the most part, the enhanced diffusion is caused by the interaction of the particles with ultralow-frequency (ULF) waves with periods, typically, of minutes. Satellite observations of a number of recent storms have shown a correlation between the amount of ULF power and the enhancement of the radiation belt fluxes (*47*, *48*). Elkington *et al.* (*49*) have shown how the asymmetric compression of the magnetosphere by the solar wind and the presence of a convection electric field can lead to an efficient resonant acceleration process by the ULF waves. Use of global MHD simulations of storm events to provide electric and magnetic fields for test-particle calculations of the radiation belts have shown responses of the radiation belts comparable to those observed on 10 and 11 January (*50*, *51*). The same combination of ULF fields estimated from MHD simulations has given similar agreement with observations for a number of recent storms (*52*).

The past decade has revealed a solar wind–magnetosphere–ionosphere system that is more dynamic than previously thought in many ways. It has also revealed the extent to which the solar wind, and ultimately the sun, control the system. The future combination of enhanced spacecraft and ground observations and advances in modeling will allow us to begin the science of space meteorology in the new decade.

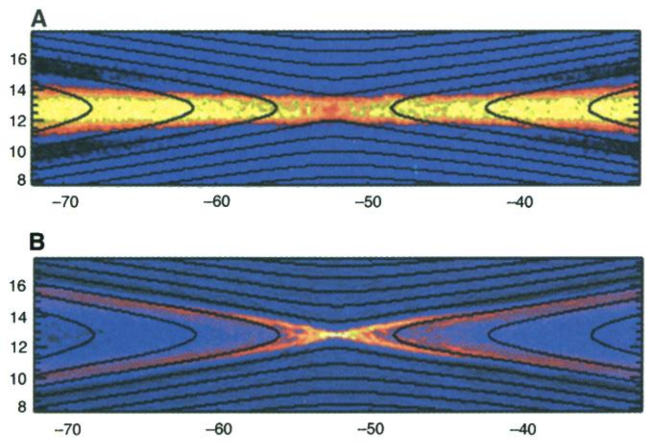

Fig. 4. The ion (**A**) and electron (**B**) current layers in a particle simulation of magnetic reconnection. The figures are false color-coded with the intensity of the current. Magnetic field lines are superimposed on the current distributions.

References and Notes

1. D. N. Baker, J. H. Allen, S. G. Kanekal, G. D. Reeves, *Eos* **79**, 477 (1998).
2. K. Sawyer, "Earth takes a 'one-two punch' from a solar magnetic cloud," *Washington Post*, 23 January 1997, p. A1.
3. R. Showstack, *Eos* **79**, 601 (1998).
4. D. N. Baker, R. D. Belian, P. R. Higbie, R. W. Klebesadel, J. B. Blake, *J. Electrostat.* **20**, 3 (1987).
5. D. N. Baker, S. Kanekal, J. B. Blake, B. Klecker, G. Rostoker, *Eos* **75**, 401 (1994).
6. Office of the Federal Coordinator, National Space Weather Plan (*FCM-P31-1997*, 1997) (available at www.ofcm.gov/nswp-ip/text/cover.htm).
7. J. E. Dungey, *Phys. Rev. Lett.* **6**, 47 (1961).
8. N. J. Fox, M. Peredo, B. J. Thompson, *Geophys. Rev. Lett.* **25**, 2461 (1998).
9. D. F. Webb, E. W. Cliver, N. Gopalswamy, H. S. Hudson, O. C. St. Cyr, *Geophys. Res. Lett.* **25**, 2469 (1998).
10. L. F. Burlaga, in *Physics of the Inner Heliosphere*, R. Schwenn and E. Marsch, Eds. (Springer-Verlag, New York, 1991), vol. 2, chap. 6.
11. L. Burlaga *et al.*, *J. Geophys. Res.* **103**, 277 (1998).
12. The ISTP program is an international collaboration to understand the sun, Earth's space environment, and their interaction primarily through the use of spaceborne instruments. In the United States, it is supported by NASA.
13. M. Nakamura, K. Seki, H. Kawano, T. Obara, T. Mukai, *Geophys. Res. Lett.* **25**, 2529 (1998).
14. G. Germany *et al.*, *Geophys. Res. Lett.* **25**, 3043 (1998).
15. The POLAR satellite is so called for its mission, to image the polar regions of the ionosphere and the high-latitude magnetosphere.
16. E. R. Sanchez, J. P. Thayer, J. D. Kelly, R. A. Doe, *Geophys. Res. Lett.* **25**, 2597 (1998).
17. G. Lu *et al.*, *J. Geophys. Res.* **103**, 11685 (1998).
18. M. G. Henderson *et al.*, *Geophys. Res. Lett.* **24**, 1167 (1997).
19. Geocorona is often used to mean the exosphere, that region of Earth's atmosphere where collisions are no longer important. It is also the ultraviolet light scattered off the exosphere.
20. H. Spence, personal communication.
21. M. F. Thomsen, J. E. Borovsky, D. J. McComas, R. C. Elphic, S. Maurice, *Geophys. Res. Lett.* **25**, 2545 (1998).
22. MHD is an extension of the compressible fluid dynamic (Euler) equations that includes magnetic forces on a neutral ionized fluid.
23. GEM is a National Science Foundation program focused on the production of a Global Circulation Model for the magnetosphere-ionosphere system.
24. J. Raeder, J. Berchem, M. Ashour-Abdalla, *J. Geophys. Res.* **103**, 14787 (1998).
25. J. A. Fedder, S. P. Slinker, J. G. Lyon, *J. Geophys. Res.* **103**, 14799 (1998).
26. R. M. Winglee, V. O. Papitashvili, D. R. Weimer, *J. Geophys. Res.* **102**, 26961 (1997).
27. C. C. Goodrich, J. G. Lyon, M. Wiltberger, R. E. Lopez, K. Papadapoulos, *Geophys. Res. Lett.* **25**, 2541 (1998).
28. P. A. Sweet, in *Electromagnetic Phenomena in Cosmical Physics*, B. Lehnert, Ed. (Cambridge Univ. Press, New York, 1958), pp. 123–129.
29. E. N. Parker, *J. Geophys. Res.* **62**, 509 (1957).
30. H. E. Petschek, in *AAS/NASA Symposium on the Physics of Solar Flares*, W. N. Ness, Ed. (NASA, Washington, DC, 1964), pp. 425–431.
31. M. E. Mandt, R. E. Denton, J. F. Drake, *Geophys. Res. Lett.* **21**, 73 (1994). Addition of resistivity based on kinetic (i.e., collective particle) processes does not change this conclusion.
32. Z. W. Ma and A. Bhattacharjee, *Geophys. Res. Lett.* **23**, 1673 (1996).
33. D. E. Biskamp, E. Schwarz, J. F. Drake, *Phys. Plasmas* **4**, 1002 (1997).
34. M. A. Shay and J. F. Drake, *Geophys. Res. Lett.* **25**, 3759 (1998).
35. M. Hesse, K. Schindler, J. Birn, M. Kuznetzova, *Phys. Plasmas* **6**, 1781 (1999).
36. M. Shay, personal communication.
37. Whistlers are electromagnetic waves in a plasma with frequencies that are too fast for the massive ions to respond but below the electron gyrofrequency. For a discussion, see, for example, W. Baumjohann and R. A. Treuman [*Basic Space Plasma Physics* (Imperial College Press, London, 1996)].
38. J. Birn *et al.*, *J. Geophys. Res.*, in press. See also P. Pritchett (*J. Geophys. Res.*, in press), M. Hesse *et al.* (*J. Geophys. Res.*, in press), M. Shay *et al.* (*J. Geophys. Res.*, in press), M. Kuznetzova *et al.* (*J. Geophys. Res.*, in press), J. Birn and M. Hesse (*J. Geophys. Res.*, in press), Z. Ma and A. Bhattacharjee (*J. Geophys. Res.*, in press), and A. Otto (*J. Geophys. Res.*, in press).
39. G. D. Reeves *et al.*, *J. Geophys. Res.* **103**, 17559 (1998).
40. R. S. Selesnick and J. B. Blake, *Geophys. Res. Lett.* **25**, 2553 (1998).
41. P. Buhler *et al.*, *Geophys. Res. Lett.* **25**, 2983 (1998).
42. X. Li *et al.*, *Geophys. Res. Lett.* **25**, 2561 (1998).
43. G. D. Reeves *et al.*, *Geophys. Res. Lett.* **25**, 3265 (1998).
44. X. Li *et al.*, *Geophys. Res. Lett.* **20**, 2423 (1993).
45. M. K. Hudson *et al.*, *Geophys. Res. Lett.* **22**, 291 (1995).
46. M. K. Hudson *et al.*, *J. Geophys. Res.* **102**, 14087 (1997).
47. D. N. Baker *et al.*, *J. Geophys. Res.* **103**, 17279 (1998).
48. D. N. Baker *et al.*, *Geophys. Res. Lett.* **25**, 2975 (1998).
49. S. R. Elkington, M. K. Hudson, A. A. Chan, *Geophys. Res. Lett.* **26**, 3273 (1999).
50. M. K. Hudson, S. R. Elkington, J. G. Lyon, C. C. Goodrich, *Adv. Space Res.* **25**, 2327 (1999).
51. M. K. Hudson, S. R. Elkington, J. G. Lyon, C. C. Goodrich, T. J. Rosenberg, in *Sun-Earth Plasma Connections*, vol. 109 of *Geophysical Monograph Series*, J. L. Burch, R. L. Carovillano, S. K. Antiochos, Eds. (American Geophysical Union, Washington, DC, 1999), pp. 171–182.
52. S. R. Elkington, personal communication.

53. I would like to thank a reviewer for helpful comments. This work was partially supported by NASA and NSF.

REVIEW

Status and Improvements of Coupled General Circulation Models

Hartmut Grassl

Coupled general circulation models (CGCMs) integrate our knowledge about atmospheric and oceanic circulation. Different versions of CGCMs are used to provide a better understanding of natural climate variability on interannual and decadal time scales, for extended weather forecasting, and for making seasonal climate scenario projections. They also help to reconstruct past climates, especially abrupt climate change processes. Model intercomparisons, new test data (mainly from satellites), more powerful computers, and parameterizations of atmospheric and oceanic processes have improved CGCM performance to such a degree that the model results are now used by many decision-makers, including governments. They are also fundamental for the detection and attribution of climate change.

Numerical models integrate our knowledge of certain fields of science, but they can only be as good as our understanding of all the processes involved. For weather and climate models, large-field experiments regarding certain processes and continuous monitoring of three-dimensional (3D) dynamical and thermodynamical structure are required to increase understanding of the variability of the system studied. For long-term simulations of global climate variability and projections of its future changes, a realistic description of all climate system components is needed. Thus, a climate model simulating decades must contain at least a 3D general circulation model (GCM) of the global atmosphere coupled to the 3D world ocean, including sea ice dynamics and a representation of land surface processes (including vegetation). Whether the dynamics of the terrestrial and marine biosphere as well as of the land cryosphere are included depends on the time scale to which such a coupled model is applied. Here I review the status and recent improvements of coupled GCMs (CGCMs) that are now not only important for policy-making but are used for the evaluation of our understanding of many climate processes. They are also applied to make predictions of climate anomalies on seasonal time scales. Thus, we must continuously evaluate and improve the CGCMs we use.

Max-Planck-Institute for Meteorology, Bundesstrasse 55, D-20146 Hamburg, Germany. E-mail: grassl@dkrz.de

Historical Development

The development of atmospheric GCMs (AGCMs) for weather forecasting since the 1950s gives a good example of the growing number of processes that need to be included and the system parts needed when forecasting time scales grow.

The weather forecasting models based on